Liquid Crystals Today

ISSN: 1358-314X (Print) 1464-5181 (Online) Journal homepage: https://www.tandfonline.com/loi/tlcy20

Advanced liquid crystal displays with supreme image qualities

Haiwei Chen & Shin-Tson Wu

To cite this article: Haiwei Chen & Shin-Tson Wu (2019) Advanced liquid crystal displays with supreme image qualities, Liquid Crystals Today, 28:1, 4-11, DOI: 10.1080/1358314X.2019.1625138

To link to this article: https://doi.org/10.1080/1358314X.2019.1625138

Published online: 15 Jul 2019.

LIQUID CRYSTALS TODAY
2019, VOL. 28, NO. 1, 4–11
https://doi.org/10.1080/1358314X.2019.1625138

Taylor & Francis
Taylor & Francis Group

RESEARCH ARTICLE

OPEN ACCESS Check for updates

Advanced liquid crystal displays with supreme image qualities

Haiwei Chen and Shin-Tson Wu

CREOL, The College of Optics and Photonics, University of Central Florida, Orlando, FL, USA

ABSTRACT

'LCD vs. OLED: who wins?' is a heated debatable question. Each technology has its own pros and cons. We review recent advances in liquid crystal displays (LCDs) from three performance metrics: response time, contrast ratio, and viewing angle, which determine the final-perceived image quality. To enhance LCD performance, ultra-low viscosity materials, quantum dots, and new device structures have been explored, and their working mechanisms investigated. Another round of LCD innovation is around the corner.

KEYWORDS

Liquid crystal display; fast response time; wide colour gamut; high contrast ratio

1. Introduction

Thin-film transistor liquid crystal displays (TFT LCDs) are ubiquitous in our daily life; their applications span from smartphones, pads, computer screens, to TVs [1–3]. However, in recent years, an organic light-emitting diode (OLED) display is emerging and growing rapidly, which starts to challenge the dominance of LCDs from all aspects [4–6]. In general, these are two completely different display technologies. 'LCD vs. OLED: who wins?' is a heated debatable question. Each technology has its own pros and cons. For example, LCDs are superior in high brightness, long lifetime, low cost, and high-resolution density. However, in terms of the image quality, LCD is generally perceived inferior to OLED, mainly due to its slower response time, lower contrast ratio, and narrower colour gamut [7].

Response time affects the motion blur, which is critical for displaying fast-moving objects in movies, gaming, and sports. OLED is a self-emissive technology with 100 μs response time. Whereas LCD is non-emissive and the image transition results from molecular reorientation. Thus, its response time is typically 5–10 ms [8]. For LCD colour gamut, the backlight source is the dominant factor. Presently, phosphor-converted white light-emitting diode (WLED) is still the major light source. With one-phosphor YAG-based WLED, LCD can get ~50% Rec. 2020; with two-phosphor KSF-based WLED, the colour gamut is improved to 70–80% Rec. 2020 [9]. In comparison, RGB OLED can easily realize >80% Rec. 2020, providing more vivid colours. Lastly, OLED can get nearly infinity-to-one contrast ratio in a perfect dark room owing to its self-emissive characteristic. On the other hand, LCD's CR depends on the device configuration, but even for the best vertical alignment (VA) mode, its CR is still limited to around 5000:1, which is far lower than OLED [7,8]. As a result, to enhance the image quality of an LCD, motion picture response time, colour gamut, and contrast ratio have to be improved substantially.

In this paper, we will review some of our recently developed LCD device structures with detailed working mechanism elucidated. These novel designs can boost the LCD's performance in response time, colour gamut, and contrast ratio to be comparable with OLED or even better.

2. Motion picture response time

As mentioned earlier, motion image blur would occur when the display response is not fast enough. To characterize image blurs, motion picture response time (MPRT) has been proposed and commonly practiced [10–13]. Previously, calculating the MPRT of an active matrix display was rather difficult, because several effects are involved, like sample-and-hold effect, image motion, and human vision effect. This task becomes incredibly simple, as *Peng et al.* derived an analytical equation to describe the MPRT [14,15]:

$$MPRT = \sqrt{\tau^2 + (0.8T_f)^2} \tag{1}$$

where T_f is the frame time (e.g. T_f= 16.67 ms for 60 fps). Using this equation, we can easily obtain MPRT as long as LC response time and TFT frame rate are known.

Figure 1 is a plot of simulated MPRT at different TFT frame rates. It is seen that at a given frame rate, say 120 fps, as the LC response time decreases, MPRT decreases almost linearly and then gradually saturates. Note that the MPRT for τ= 2 ms is only 4% longer than that of τ= 0 (i.e. 6.96 ms vs. 6.67 ms). Therefore, if an LCD's response

CONTACT Haiwei Chen haiwei.chen@knights.ucf.edu

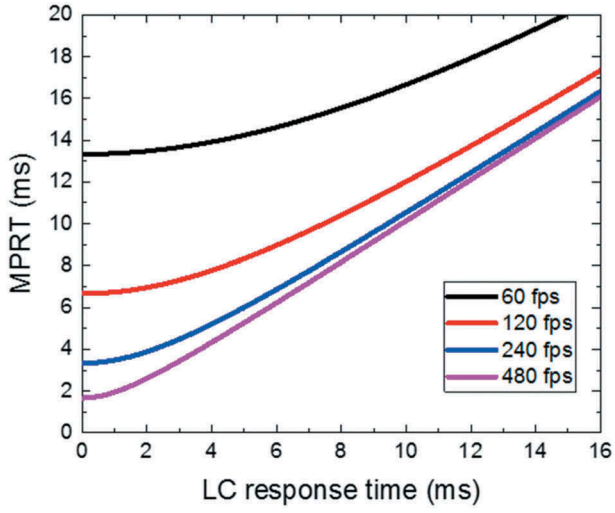

Figure 1. Calculated MPRT as a function of LC (or OLED) response time at different frame rates.

Reproduced from Ref. [14], with the permission of AIP Publishing.

time is 2 ms or less, then its MPRT is comparable to that of an OLED display, even if the OLED's response time is assumed to be 0.

In practice, we do not need to keep pushing LC response time to zero; instead, 2 ms is minimally acceptable from the theoretical predications shown in Figure 1. To achieve this goal ($\tau \leq 2$ ms), in the following sections, we will focus on three approaches by using 1) ultra-low viscosity LC mixtures, 2) new LCD structure design, e.g. single-rubbing vertical alignment fringe in-plane switching, and 3) new LCD operation mode, e.g. polymer-stabilized blue phase liquid crystal.

2.1. Fast-response LCD with ultra-low viscosity LC mixtures

The response time of an LCD is governed by the cell gap, rotational viscosity (γ_1), and elastic constant of the employed LC material. Here, we developed an ultra-low viscosity LC mixture with negative dielectric anisotropy ($\Delta\varepsilon < 0$), called MX-40593 [15]. Its physical properties are listed in Table 1, where the rotational viscosity is only 59.5 mPas, about twice lower than other typical negative $\Delta\varepsilon$ LC mixtures.

Next, we injected MX-40593 into a commercial VA cell with a cell gap $d = 3.3$ μm and measured its grey-to-grey (GTG) response time. During the measurement, we

Table 1. Measured physical properties of MX-40593. $T = 22$°C and $\lambda = 633$ nm.

Δn	$\varepsilon_{//}$	$\varepsilon_{\perp}$	Δε	K_{33} (pN)	γ_1/K_{33} (ms/μm^2)	γ_1 (mPas)	T_c (°C)
0.098	3.41	5.88	−2.47	11.9	5.0	59.5	79.3

Table 2. Measured GTG response time of our VA cell with overdrive and undershoot. $d = 3.3$ μm, $\lambda = 633$ nm and $T = 22$°C.

	1	2	3	4	5	6	7	8
1		0.58	0.70	0.72	0.93	0.96	1.02	1.37
2	2.73		0.12	0.23	0.34	0.51	0.70	1.14
3	2.81	1.14		0.12	0.27	0.41	0.62	1.05
4	3.56	1.44	0.55		0.13	0.28	0.49	1.01
5	3.73	2.07	1.09	0.54		0.13	0.34	0.98
6	4.07	2.49	1.54	0.92	0.40		0.22	0.87
7	4.23	2.94	2.01	1.41	0.82	0.33		0.69
8	4.61	3.24	2.40	1.84	1.28	0.82	0.39	

applied overdrive and undershoot voltages to accelerate the transition process [16]. From Table 2, the average GTG response time is 1.29 ms. As mentioned earlier, the MPRT of an LCD would be comparable to that of an OLED, as long as the LC response time is 2 ms or less. To validate this finding, we measured the GTG MPRT using our MX-40593 at $f = 120$ Hz, and the obtained average GTG MPRT is 6.88 ms, while it is 6.67 ms for OLED. In other words, LCD and OLED indeed show comparable motion image blur.

2.2. Fast-response LCD with advanced structure design

In addition to material development, several LCD structures have been proposed to improve the response time, for examples, thin cell gap [17,18], triode electrode [19–21], dual fringe field switching (FFS) [22], etc. Here, we focus on a new design, called single-rubbing vertical-alignment fringe in-plane switching (VA-FIS) [23].

Figure 2 depicts the schematic diagram. Please note that there is only one alignment layer on the top glass substrate to induce vertical alignment at the voltage-off state. Meanwhile, the planar electrode on the top substrate is with a fixed voltage (or biased voltage V_{bias}). Combined with the bottom common electrode ($V_{com} = 0$), a strong longitudinal electric field is produced in the whole panel. This has two effects: 1) the LC directors are vertically aligned along the electric field direction, leading to a high contrast ratio; 2) the

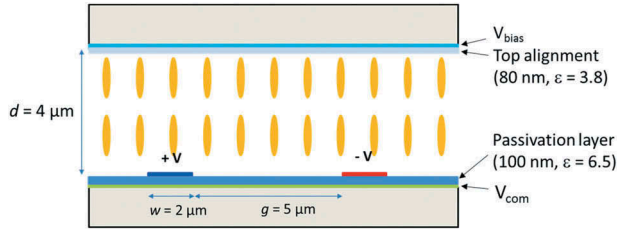

Figure 2. Schematic diagram of the proposed single-rubbing VA-FIS mode.

Reproduced from Ref. [23], with the permission of The Society for Information Display.

LC directors are pulled back by the longitudinal field to their initial state when the horizontal electric field is removed, leading to fast decay time.

Compared to conventional double-rubbing VA-FIS, the newly proposed single-rubbing design shows significant improvement [Figure 3]. For example, its VT curve climbs up much earlier and faster. The corresponding on-state voltage is only 17 V, and the transmittance at 15 V is as high as 69.3%. Meanwhile, the rise time of such a VA-FIS cell is $\tau_{on} = 0.91$ ms and decay time is $\tau_{off} = 0.93$ ms. This is much faster than the required 2 ms. In fact, if we adopt the overdrive and undershoot driving method, the average GTG response time is reduced to ~0.4 ms. Moreover, all the greyscale transitions are below 1 ms, which is highly desirable for suppressing motion blurs.

2.3. Fast-response blue-phase LCD

Although nematic liquid crystal is the mainstream for present display applications, other new LC modes, such as ferroelectric liquid crystal [24–26] and blue phase liquid crystal (BPLC) [27–29], have also been explored extensively. Both of them can get sub-millisecond response time, due to their unique LC arrangement and orientations. Here, we use polymer-stabilized BPLC as an example, which is optically isotropic and has no need for surface alignment. The biggest drawback for polymer-stabilized BPLC is its relatively high operation voltage [30].

To lower the operation voltage, we proposed a new-protruded diamond-shape in-plane-switching (DIPS) electrode configuration, as shown in Figure 4 [31]. The conventional strip protrusion is modified to diamond shape so that the effective dead zone area can be greatly reduced. Compared to conventional protruded IPS [Figure 5], the on-state voltage of DIPS is lowered by 41.4% (from 26.1 V to 15.3 V) while keeping the same transmittance (75.5%). More importantly, these results are realized by using an industrially proven blue phase material, which processes sub-millisecond response, good long-term stability, no TFT charging issue, and high voltage holding ratio.

3. Wide colour gamut

Vivid colour is a desirable trait in all visual displays, including LCDs. To improve colour performance, a straightforward way is to narrow the backlight's spectral bandwidth. This is because of the better purity of red, green, and blue (RGB) lights. In the past two decades, the bandwidth of the LCD backlight has been decreased from 120 nm to 20 nm, i.e. from YAG WLED, to KSF WLED and then to quantum dots (QDs) [9,32]. The corresponding colour gamut is increased from 50% Rec. 2020 to about 90% Rec. 2020. Unfortunately, below 20 nm, continuing to narrow the bandwidth becomes prohibitively difficult, so that the colour gamut improvement is almost halting.

To understand the underlying mechanisms, we investigate colour gamut and total light efficiency (TLE) and plot the results in Figure 6 [33]. Here, TLE is defined as:

$$TLE = \frac{K_m \int S_{out}(\lambda) V(\lambda) d\lambda}{\int S_{in}(\lambda) d\lambda}, \tag{2}$$

where S_{in} (λ)/S_{out} (λ) is the spectral power distribution (SPD) of the input/output light, $V(\lambda)$ is the standard luminosity function, and K_m = 683 lm/W is the *luminous efficacy of radiation* of an ideal monochromatic 555-nm source. In the calculation, a commercially available high-efficient colour gamut is employed [33–35].

From Figure 6, several interesting phenomena are found. Firstly, there exists an inherent trade-off between light efficiency and colour gamut. Thus, a delicate balance should be chosen in practical applications. Secondly, for backlight with the same FWHM, there is indeed a theoretical limit for the colour gamut.

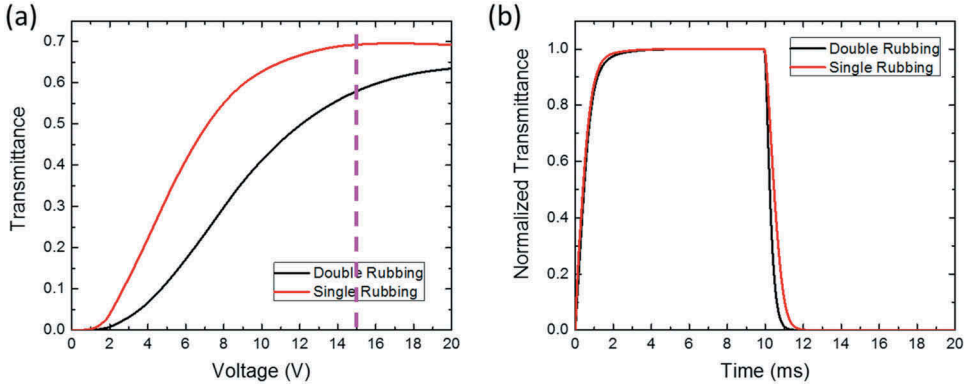

Figure 3. Simulated (a) VT and (b) TT curves for VA-FIS with and without bottom alignment layer. (λ = 550 nm. Here, polyimide alignment layer is used with 70 nm thick).

Reproduced from Ref. [23], with the permission of The Society for Information Display.

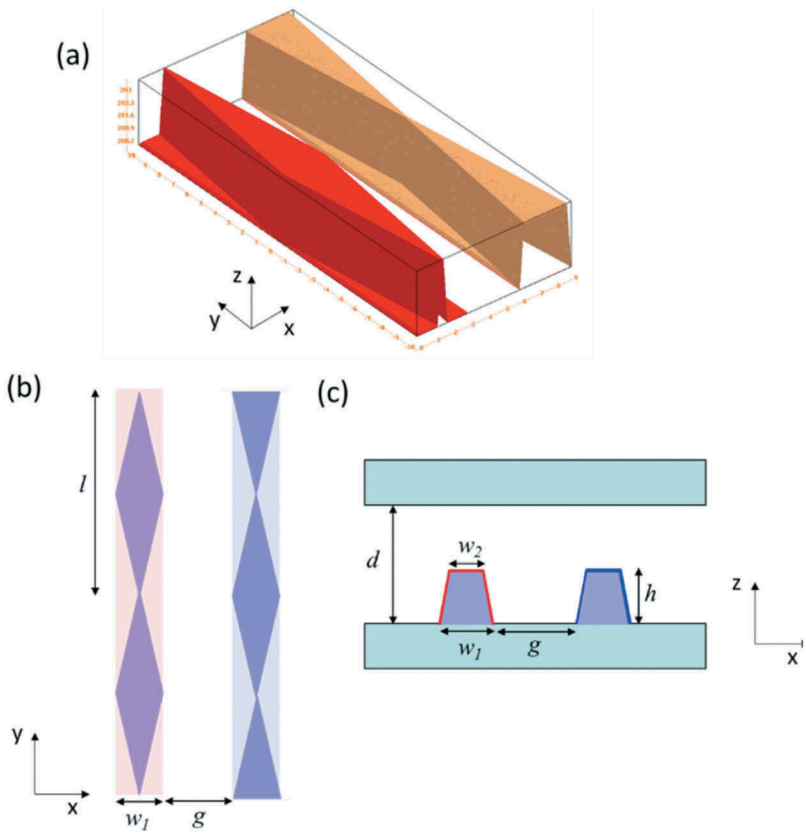

Figure 4. (a) Schematic 3D diagram of the proposed DIPS structure; (b) top view and (c) cross-section view.
Reproduced from Ref. [31], with the permission of Taylor & Francis Group.

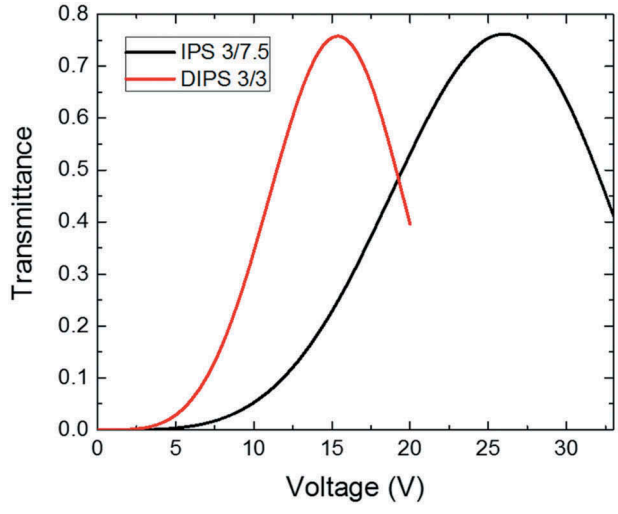

Figure 5. Simulated VT curves for conventional IPS and DIPS. (w_1 = 3 μm, w_2 = 2.5 μm, g= 7.5 μm, h = 3.5 μm, and d= 9 μm for IPS; w_1 = 3 μm, w_2 = 2.5 μm, g= 3 μm, h = 3.5 μm, d= 9 μm, and l= 20 μm for DIPS).
Reproduced from Ref. [31], with the permission of Taylor & Francis Group.

For example, when the FWHM of a light source is 30 nm, the largest achievable colour gamut is 90.1% Rec. 2020 in CIE 1931 [Figure 6(a)] or 91.5% Rec. 2020 in CIE 1976 [Figure 6(b)]. Next, we find that as the light source becomes more saturated (i.e. narrower FWHM), the maximum colour gamut increases and then gradually saturates. From 30-nm to 20-nm FWHM, according to Figure 6, the colour gamut improvement is only 2%. Even if the FWHM of the light emitters were laser-like (≤1 nm), the maximum colour gamut is ~93.5% Rec. 2020. This limits the colour gamut that an LCD can possibly achieve.

To go beyond this limit, a new backlight configuration is proposed as Figure 7 depicts. The key components are a functional reflective polarizer (FRP) and a patterned half-wave plate. FRP is a multi-layer structure with alternative refractive indices (n_1 and n_2). It functions as a band-pass filter for both polarization directions: For x-polarized incident light, only the blue wavelength could pass, whereas the rest is reflected. For y-polarized incident light, it is reversed: only green and red lights could pass through FRP, while blue light is reflected. Above FRP is a patterned phase retardation film, which is divided into half-wave region and free region. For the light traversing through the λ/2 region, its polarization is rotated by 90°, e.g. x-polarization turns to y-polarization or vice versa. If the light passes

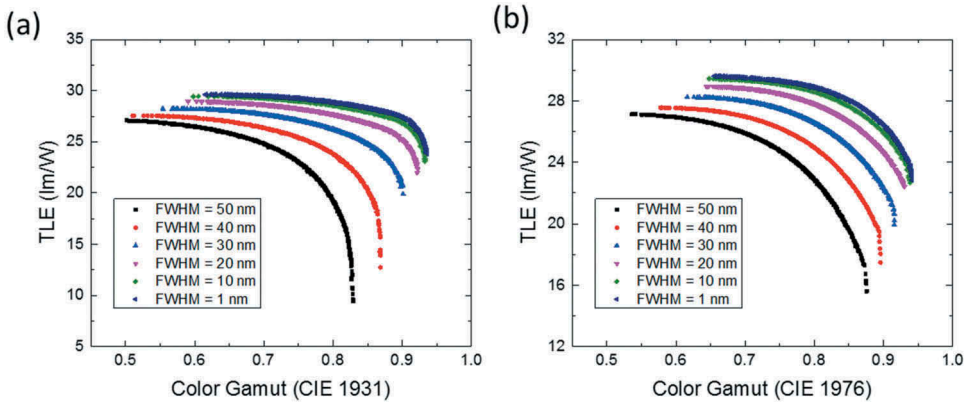

Figure 6. Pareto front defined in (a) CIE 1931 and (b) CIE 1976 with different FWHM light sources.
Reproduced from Ref. [33], with the permission of Springer Nature.

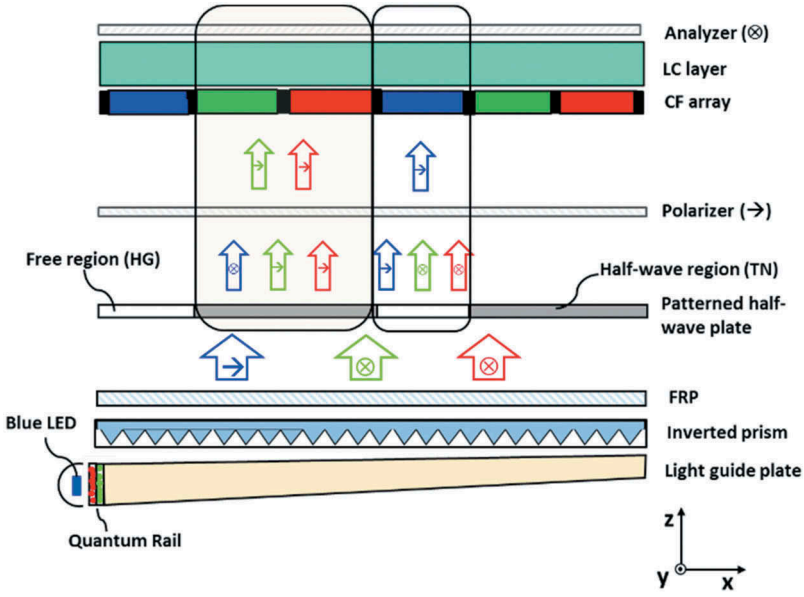

Figure 7. Schematic diagram and working principle of the proposed backlight with a functional reflective polarizer (FRP) and a patterned half-wave plate. (TN: twisted nematic alignment; HG: homogeneous alignment).
Reproduced from Ref. [33], with the permission of Springer Nature.

through the free region, then its polarization remains unchanged.

From system perspective, as shown in Figure 7, only blue light can enter the blue sub-pixels, because green/red lights are absorbed by the linear polarizer due to mismatched polarization. Similar situation occurs to the green and red sub-pixels. Therefore, *no crosstalk* exists between the blue and green/red regions, leading to a much wider colour gamut. In experiment, a colour gamut of 97.3% Rec. 2020 in CIE 1976 has been realized, a measurement on par with those attained by laser projectors.

4. High contrast ratio

High contrast ratio (CR) is another equally important parameter to achieve supreme image quality. However, for a non-emissive LCD, its CR is inherently limited, due to the unwanted light leakage at voltage-off state. Currently, a commercial VA LCD TV only shows CR ~ 5000:1. The main root cause for such a low contrast is the so-called depolarization effect inside an LCD panel [36–40], including diffraction effect, scattering effect, misalignment effect, etc.

To mitigate the effect of depolarization, a new device structure has been proposed, as Figure 8 depicts, by adding an in-cell polarizer between the LC layer and the colour

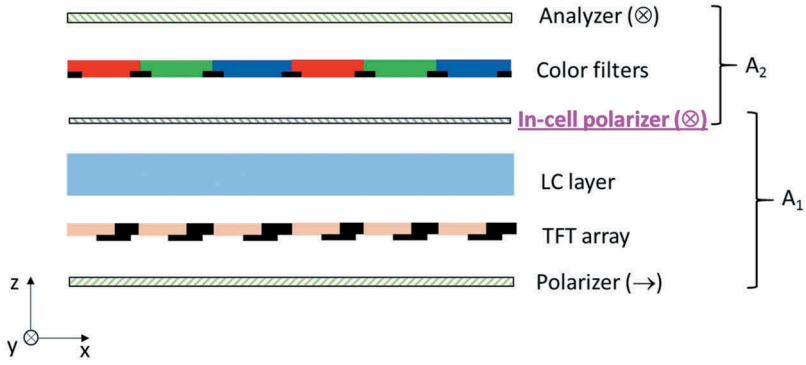

Figure 8. Schematic diagram of the proposed device structure with an in-cell polarizer.
Reproduced from Ref. [41], with the permission of The Optical Society.

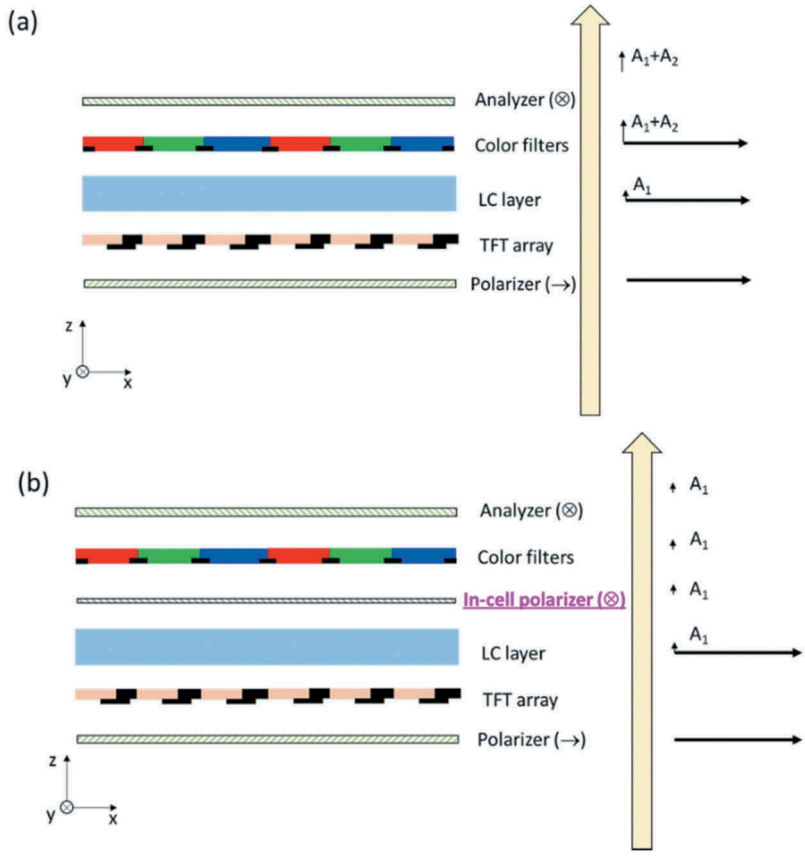

Figure 9. Working mechanism of (a) conventional LCD panel with depolarization effects, and (b) the proposed LCD panel with decoupled depolarization effects.
Reproduced from Ref. [41], with the permission of The Optical Society.

filters [41]. Because of the introduction of in-cell polarizer, the depolarization coefficients for each layer are decoupled. That is to say, below the in-cell polarizer, depolarization is mainly from TFT substrate and LC layer, which is marked as A_1; while above the in-cell polarizer, depolarization is mainly governed by the scattering effect of colour filter pigment, marked as A_2. Then, A_1 and A_2 should be treated separately, as will be discussed later.

For conventional LCD architecture [Figure 9(a)], the incoming-polarized light, say along the x-axis, goes through the TFT substrate and LC layer, there is some light leakage along y-axis due to scattering effect. Here, it is governed by A_1. After the light passing through colour filters, the depolarization becomes more severe, represented by A_1+ A_2. When entering the analyser, the x-polarized (dominant polarization direction) light is

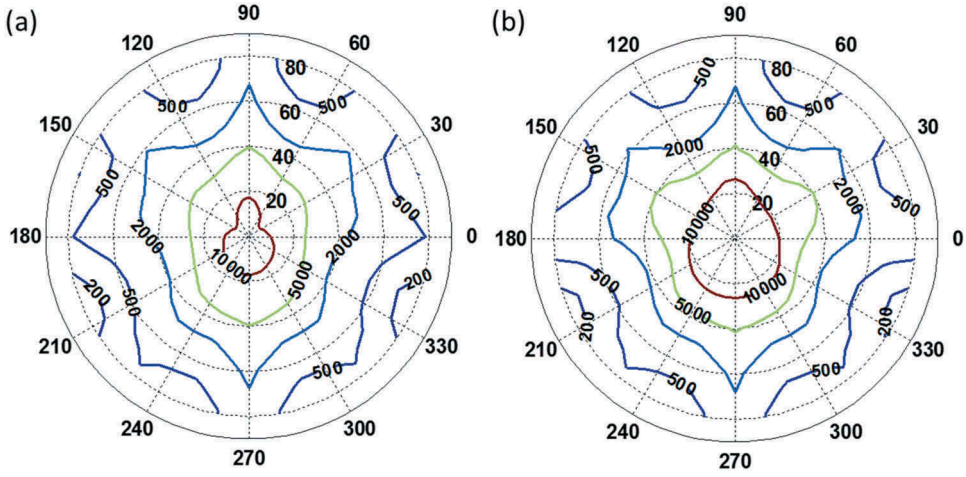

Figure 10. Simulated isocontrast contour for the proposed device configuration in MVA mode. (a) Polarizer thickness is 24 μm, and (b) Polarizer thickness is 29 μm. For the 24-μm thick polarizer: CR_{max}= 12,277:1, CR_{min}= 132:1, and CR_{ave} = 4685:1. For the 29 μm thick polarizer: CR_{max} = 23,163:1, CR_{min} = 149:1, and CR_{ave} = 7223:1.
Reproduced from Ref. [41], with the permission of The Optical Society.

blocked as expected, while only the depolarized light (jointly determined by A_1+ A_2) could traverse through the analyser. This undesirable light leakage degrades the contrast ratio.

For the proposed device structure [Figure 9(b)], the depolarization effect remains the same for the TFT substrate and LC layer, which is A_1. But above the LC layer, there is an in-cell polarizer to absorb the x-polarized light; only the scattered light could leak through and enter the colour filter array (although it has a strong scattering effect). In this case, the depolarized light is still governed by A_1, and it becomes the final light leakage. Therefore, the effective CR would be enhanced greatly.

Figure 10 shows the simulated viewing angle of a new multi-domain VA (MVA) mode. For conventional 24 μm thick polarizer [Figure 10(a)], the maximum CR is improved from 5000:1 to 12,277:1, which is about 2.4x higher. In addition, the high CR region is greatly widened, and the average CR for the entire viewing zone is >4,500:1. If we slightly increase the polarizer thickness to 29 μm [Figure 10 (b)], the maximum CR is improved to 23,163:1. This is a record-high CR for LCD. To enhance an LCD's CR further, local dimming backlight could be implemented [42–45]. By tailoring the brightness of segmented backlight, the dynamic CR could be boosted to 1,000,000:1.

5. Conclusion

We have reviewed recent progress on liquid crystal displays from three key display metrics: fast response time, wide colour gamut, and high contrast ratio, which affect the final-perceived image quality. Firstly, we investigate how response time affects the motion blur, and then discover the 2-ms rule. With ultra-low viscosity material, advanced structure design, and new operation mode, LCDs with comparable MPRT to OLED displays can be realized. Next, we propose a novel backlight configuration to improve an LCD's colour gamut. A functional reflective polarizer (FRP) is working with a patterned half-wave plate to suppress the crosstalk between blue and green/red lights. In experiment, 97.3% Rec. 2020 in CIE 1976 colour space is achieved, which is approaching the colour gamut of a laser projector. Finally, to enhance an LCD's contrast ratio, a novel device configuration is proposed by adding an in-cell polarizer between LC layer and colour filter array. The CR of a VA LCD is improved from 5000:1 to 20,000:1. To enlarge CR to 1,000,000:1, local dimming backlight could be implemented. Along with other outstanding features, like high peak brightness, high-resolution density, long lifetime, and low cost, LCD would continue to maintain its dominance in the foreseeable future.

Disclosure statement

No potential conflict of interest was reported by the authors.

References

[1] Castellano JA, ed. Handbook of display technology. Amsterdam: Elsevier; 2012.
[2] Schadt M. Milestone in the history of field-effect liquid crystal displays and materials. Jpn J Appl Phys. 2009;48:03B001.
[3] Ukai Y. TFT-LCDs as the future leading role in FPD. SID Symp Dig Tech Pap. 2013;44:28–31.
[4] Tang CW, VanSlyke SA. Organic electroluminescent diodes. Appl Phys Lett. 1987;51:913–915.

[5] Geffroy B, Le Roy P, Prat C. Organic light-emitting diode (OLED) technology: materials, devices and display technologies. Polym Int. 2006;55:572–582.
[6] Buckley A. Organic light-emitting diodes (OLEDs): materials, devices and applications. Amsterdam: Elsevier; 2013.
[7] Chen H, Lee JH, Lin BY, et al. Liquid crystal display and organic light-emitting diode display: present status and future perspectives. Light Sci Appl. 2018;7:17168.
[8] Yang DK, Wu ST. Fundamentals of liquid crystal devices. 2nd ed. New York: John Wiley & Sons; 2014.
[9] Chen H, He J, Wu ST. Recent advances on quantum-dot-enhanced liquid crystal displays. IEEE J Sel Topics Quantum Electron. 2017;23:1900611.
[10] Yamamoto T, Aono Y, Tsumura M. Guiding principles for high quality motion picture in AMLCDs applicable to TV monitors. SID Symp Dig Tech Pap. 2000;31:456–459.
[11] Kurita T. Moving picture quality improvement for hold-type AM-LCDs. SID Symp Dig Tech Pap. 2001;32:986–989.
[12] Igarashi Y, Yamamoto T, Tanaka Y, et al. Summary of moving picture response time (MPRT) and futures. SID Symp Dig Tech Pap. 2004;35:1262–1265.
[13] Someya J, Sugiura H. Evaluation of liquid-crystal-display motion blur with moving-picture response time and human perception. J Soc Inf Disp. 2007;15:79–86.
[14] Peng F, Chen H, Gou F, et al. Analytical equation for the motion picture response time of display devices. J Appl Phys. 2017;121:023108.
[15] Chen H, Peng F, Gou F, et al. Nematic LCD with motion picture response time comparable to organic LEDs. Optica. 2016;3:1033–1034.
[16] Wu ST. Nematic liquid crystal modulator with response time less than 100 μs at room temperature. Appl Phys Lett. 1990;57:986–988.
[17] Ge Z, Wu ST, Kim SS, et al. Thin cell fringe-field-switching liquid crystal display with a chiral dopant. Appl Phys Lett. 2008;92:181109.
[18] Chen H, Luo Z, Xu D, et al. A fast-response A-film-enhanced fringe field switching liquid crystal display. Liq Cryst. 2015;42:537–542.
[19] Channin DJ. Triode optical gate: a new liquid crystal electro-optic device. Appl Phys Lett. 1975;26:603.
[20] Xiang CY, Guo JX, Sun XW, et al. A fast response, three-electrode liquid crystal device. Jpn J Appl Phys. 2003;42:L763–765.
[21] Kim JW, Choi TH, Yoon TH. Fast switching of nematic liquid crystals over a wide temperature range using a vertical bias electric field. Appl Opt. 2014;53:5856–5859.
[22] Jiao MZ, Ge ZB, Wu ST, et al. Submillisecond response nematic liquid crystal modulators using dual fringe field switching in a vertically aligned cell. Appl Phys Lett. 2008;92:111101.
[23] Chen H, Huang Y, Gou F, et al. New nematic LCD with submillisecond response time. SID Symp Dig Tech Pap. 2018;49:1691–1694.
[24] Beresnev LA, Chigrinov VG, Dergachev DI, et al. Deformed helix ferroelectric liquid crystal display: a new electrooptic mode in ferroelectric chiral smectic C liquid crystals. Liq Cryst. 1989;5(4):1171–1177.
[25] Zhang YS, Liu CY, Emelyanenko AV, et al. Synthesis of predesigned ferroelectric liquid crystals and their applications in field-sequential color displays. Adv Funct Mater. 2018;28:1706994.
[26] Shi L, Srivastava AK, Cheung A, et al. Active matrix field sequential color electrically suppressed helix ferroelectric liquid crystal for high resolution displays. J Soc Inf Disp. 2018;26:325–332.
[27] Kikuchi H, Yokota M, Hisakado Y, et al. Polymer-stabilized liquid crystal blue phases. Nat Mater. 2002;1:64.
[28] Ge Z, Gauza S, Jiao M, et al. Electro-optics of polymer-stabilized blue phase liquid crystal displays. Appl Phys Lett. 2009;94:101104.
[29] Yan J, Cheng HC, Gauza S, et al. Extended Kerr effect of polymer-stabilized blue-phase liquid crystals. Appl Phys Lett. 2010;96:071105.
[30] Huang Y, Chen H, Tan G, et al. Optimized blue-phase liquid crystal for field-sequential-color displays. Opt Mater Express. 2017;7:641–650.
[31] Chen H, Lan YF, Tsai CY, et al. Low-voltage blue-phase liquid crystal display with diamond-shape electrodes. Liq Cryst. 2017;44:1124–1130.
[32] Chen J, Hardev V, Hartlove J, et al. High-efficiency wide-color-gamut solid-state backlight system for LCDs using quantum dot enhancement film. SID Symp Dig Tech Pap. 2012;43(1):895–896.
[33] Chen H, Zhu R, He J, et al. Going beyond the limit of an LCD's color gamut. Light Sci Appl. 2017;6:e17043.
[34] Luo Z, Xu D, Wu ST. Emerging quantum-dots-enhanced LCDs. J Disp Technol. 2014;10:526–539.
[35] Zhu R, Luo Z, Chen H, et al. Realizing rec. 2020 color gamut with quantum dot displays. Opt Express. 2015;23:23680–23693.
[36] Utsumi Y, Kajita D, Takeda S, et al. Correlation of light scattering of homogenous alignment liquid crystal layers with material properties of liquid crystals. Jpn J Appl Phys. 2008;47:2205–2208.
[37] Hsu JS, Lin YH, Lin HC, et al. Thermally induced light leakage in in-plane-switching liquid crystal displays. J Appl Phys. 2009;105:033503.
[38] Takemoto H, Fuchida T, Miyatake M. Analysis of depolarized light-scattering in LCD panel and proposal of LCD systems for enhancing contrast ratio. SID Symp Dig Tech Pap. 2009;40:514–517.
[39] Utsumi Y, Takeda S, Kagawa H, et al. Improved contrast ratio in IPS-Pro LCD TV by using quantitative analysis of depolarized light leakage from component materials. SID Symp Dig Tech Pap. 2008;39:129–132.
[40] Kim KJ, Lee TR, Son HH, et al. Realization of true black quality in in-plane switching mode for LCD TV applications. SID Symp Dig Tech Pap. 2010;41:487–490.
[41] Chen H, Tan G, Li MC, et al. Depolarization effect in liquid crystal displays. Opt Express. 2017;25:11315–11328.
[42] Chen H, Sung J, Ha T, et al. Backlight local dimming algorithm for high contrast LCD-TV. Proc ASID. 2006;6:168–171.
[43] Lin FC, Huang YP, Liao LY, et al. Dynamic backlight gamma on high dynamic range LCD TVs. J Disp Technol. 2008;4:139–146.
[44] Chen H, Ha TH, Sung JH, et al. Evaluation of LCD local-dimming-backlight system. J Soc Inf Disp. 2010;18:57–65.
[45] Yoo O, Nam S, Choi J, et al. Contrast enhancement based on advanced local dimming system for high dynamic range LCDs. SID Symp Dig Tech Pap. 2017;48:1667–1669.